

Three-Dimensional Quantitative Structure-Activity Relationships of 5-HT Receptor Binding Data for Tetrahydropyridinylindole Derivatives: A Comparison of the Hansch and CoMFA Methods

Atul Agarwal,^{†,§} Philip P. Pearson,[†] Ethan Will Taylor,[†] Hong B. Li,[‡] Torsten Dahlgren,[‡] Margareta Herslöf,[‡] Youhua Yang,[‡] Georgina Lambert,[‡] David L. Nelson,[†] John W. Regan,[‡] and Arnold R. Martin^{*‡}

Department of Medicinal Chemistry, College of Pharmacy, The University of Georgia, Athens, Georgia 30602, and Department of Pharmacology and Toxicology, College of Pharmacy, University of Arizona, Tucson, Arizona 85621

Received May 25, 1993[®]

A series of new derivatives of 3-(1,2,5,6-tetrahydropyridin-4-yl)indole (4-THPI) has been synthesized, and their dissociation constants at the 5-HT_{1A} and 5-HT₂ serotonin (5-HT) receptor subtypes have been determined. The new data were combined with similar binding data on a related set of THPI analogs reported previously (Taylor *et al. Mol. Pharmacol.* 1988, 34, 42-53) and used to develop 3-dimensional quantitative structure-activity relationships (3-D QSARs) for these compounds at the 5-HT_{1A} and 5-HT₂ receptor sites, by the method of comparative molecular field analysis (CoMFA). Since the previous study included several conventional QSARs obtained by Hansch analysis, and the new compounds in some cases fall within the congeneric series used in those analyses, we were able to make a direct comparison of the predictive capabilities of CoMFA and Hansch analysis using identical training and test data sets. The overall quality of actual predictions of activity by both methods appears to be about the same, as assessed by the root mean square (rms) residuals between actual and predicted pK_i values. On the one hand, the compounds most poorly predicted by the Hansch analysis were 34, 35, and 37, while compounds 30-33 were relative poorly predicted by CoMFA. However, a clear advantage of CoMFA is the ability to include diversely substituted or noncongeneric analogs that must be omitted from conventional QSAR analysis. Using the entire data set of 45 THPI analogs reported here, pK_i predictions for six additional compounds having 5-heteroarylindole substituents gave rms residuals of 0.46 and 0.36 for the 5-HT_{1A} and 5-HT₂ models, respectively; this is close to the experimental error of the binding data. The significance of the CoMFA field graphs in terms of molecular features required for activity and selectivity at these 5-HT receptor subtypes is discussed.

Introduction

The 3-(1,2,5,6-tetrahydropyridin-4-yl)indoles (4-THPI) represent a group of semirigid analogs of serotonin (5-hydroxytryptamine, 5-HT), possessing the inherent property of acting on serotonergic systems. They are an interesting series of compounds in which to study the effects of different substituents on 5-HT receptor binding, since as a class they seem to fit the structural requirements for recognition at serotonin receptors and have the added benefit of being relatively easy to synthesize.

The pharmacological actions of 5-HT can be attributed to interactions of its indole ring and alkylamino side chain with various 5-HT receptors. Thus, the orientation of the alkyl side chain and its basic amino nitrogen may be of prime importance in accounting for recognition at different 5-HT receptor subtypes. The 4-THPI provide a partially fixed conformation of the amino group because of its inclusion in the tetrahydropyridine ring (see figures in key to Table I). Although there is a rotatable bond between the indole 3-carbon and the pyridine moiety, this bond is somewhat constrained to near-planar conformations because of conjugation between the indole ring and the double bond of the tetrahydropyridine. Thus, a coplanar conformation between these two components of 4-THPI is favored. In the absence of this double bond, the saturated

pyridine ring (piperidine) is relatively noncoplanar with the indole ring system.

The prototype for this series of compound, RU 24969 (1, Table I), is the most thoroughly investigated of a number of derivatives of 4-THPI that have been previously examined for dopaminergic and 5-HT agonist activity.¹⁻⁴ Binding studies suggest that RU 24969 is relatively selective for 5-HT_{1A} and 5-HT_{1B} sites^{5,6} with lesser activity at 5-HT_{1C}, 5-HT₂, and 5-HT_{1D} sites.^{5,6}

In a previous study,⁷ we used a series of 4-THPI analogs to investigate steric, electronic and hydrophobic requirements for recognition at 5-HT_{1A} and 5-HT₂ receptor binding sites. In that study, the pK_i values of different analogs were quantitatively related to various structural descriptors by applying a modified Hansch approach to a set of over 25 substituted 4-THPI. The results suggested that, within the series of analogs examined, it is the volume of the indole 5-substituent which almost exclusively determines the potency for 5-HT_{1A} sites, the optimal size being about 24 Å³ (calculated by fitting the activity vs volume data to a bilinear function). However, a balance of the smallest possible volume and the greatest possible hydrophobicity at the indole 5-position is required for maximal potency at 5-HT₂ sites. Although statistically less significant, a minor electronic contribution to the QSARs involving the charge on the indole 5-carbon was found to be of opposite sign for 5-HT_{1A} vs 5-HT₂ sites. The results also suggested that the indole and tetrahydropyridine rings are most likely to be in a coplanar conformation when binding at both 5-HT_{1A} and 5-HT₂ sites.

* To whom correspondence should be addressed.

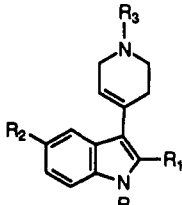
[†] The University of Georgia.

[‡] University of Arizona.

[§] Current address: Boehringer Ingelheim Pharmaceuticals, Inc., Research and Development, 175 Briar Ridge Road, Ridgefield, Ct 06877.

[®] Abstract published in *Advance ACS Abstracts*, November 1, 1993.

Table I. 5-HT Binding Data and CoMFA Predictions for 3-(Tetrahydropyridin-4-yl)indole Derivatives



compd	substituents				actual vs fitted pK ₁ values			
	R	R ₁	R ₂	R ₃	5-HT _{1A}	FIT _{1A}	5-HT ₂	FIT ₂
1	H	H	OCH ₃	H	7.960	7.721	6.040	6.139
2	H	H	H	H	6.723	7.008	6.691	6.856
3	H	H	NO ₂	H	7.192	7.640	6.785	6.702
*4	H	H	H	CH ₃	6.836	6.890	7.174	7.044
*5	H	H	OCH ₃	CH ₃	7.676	7.602	6.047	6.323
*6	H	H	OH	CH ₃	7.210	7.157	6.449	6.775
*7	H	H	Br	CH ₃	7.960	7.069	7.320	7.221
*8	H	H	Cl	CH ₃	6.723	7.287	7.292	7.878
*9	H	H	F	CH ₃	7.192	7.069	7.349	7.221
*10	H	H	CH ₃	CH ₃	6.836	7.279	6.903	6.737
*11	H	H	NO ₂	CH ₃	7.676	7.519	7.063	6.888
*12	H	H	OOCCH ₃	CH ₃	7.094	7.406	6.254	5.755
*13	H	H	OCH ₂ C ₆ H ₅	CH ₃	6.955	6.850	6.401	6.389
*14	H	H	CONH ₂	CH ₃	8.276	7.839	4.774	5.701
*15	H	H	COOCH ₃	CH ₃	7.712	7.546	5.436	5.278
*16	H	H	COOC ₂ H ₅	CH ₃	7.442	7.606	5.360	5.294
*17	H	H	CN	CH ₃	7.260	7.260	6.020	6.532
*18	H	H	phthalimido	CH ₃	6.424	6.577	4.967	5.775
19	H	H	H	CH ₂ C ₆ H ₅	6.035	5.879	7.361	7.303
20	H	CH ₃	H	CH ₃	5.748	5.798	6.061	6.274
21	H	CH ₃	OCH ₃	CH ₃	6.462	6.412	5.364	5.162
22	CH ₂ C ₆ H ₅	H	H	CH ₃	5.000	4.941	7.812	7.373
23					6.289	6.048	7.714	6.933
24					6.862	6.868	6.228	5.983
25					6.264	6.242	6.543	6.764
26					5.257	5.978	5.827	5.901
27	H	H	COCH ₃	CH ₃	7.638	7.525	5.867	6.236
28	H	H	CH ₂ OH	CH ₃	6.900	7.477	5.762	5.586
29	H	H	CH(OH)CH ₃	CH ₃	6.656	6.957	5.509	6.016
30	H	H	C(OH)(CH ₃) ₂	CH ₃	6.728	6.826	5.291	5.946
31	H	H	NHCOCH ₃	CH ₃	7.114	7.404	5.000	4.910
32	H	H	NHSO ₂ CH ₃	CH ₃	6.157	6.107	4.272	4.163
33	H	H	SCH ₃	CH ₃	7.638	7.516	6.921	6.300
34	H	H	SOCH ₃	CH ₃	6.983	7.218	5.616	5.722
35	H	H	SO ₂ CH ₃	CH ₃	6.726	6.801	5.200	5.938
36	H	H	Si(CH ₃) ₃	CH ₃	6.783	6.493	6.662	5.948
37	H	H	dioxolanyl	CH ₃	7.056	7.336	6.695	6.204
38	H	H	H	n-C ₃ H ₇	6.255	6.077	6.836	6.544
39	H	H	OCH ₃	n-C ₃ H ₇	6.435	6.753	5.840	5.909
40	H	H	CONH ₂	n-CH ₃ H ₇	7.770	7.023	5.289	5.199
41	H	H	CO ₂ CH ₃	n-C ₂ H ₇	6.416	6.730	5.301	4.774
42	H	H	CN	n-C ₃ H ₇	6.519	6.531	6.019	6.385
43	H	H	NHCOCH ₃	n-C ₃ H ₇	7.432	6.727	4.301	4.699
44	H	H	C ₆ H ₅	CH ₃	7.260	7.032	5.957	5.750
45					5.627	5.614	6.670	6.667

Due to the inherent limitations of Hansch analysis, several compounds had to be omitted from the above mentioned QSAR study because they had unique substituents at positions which were not substituted in any other compounds. In the present study, the 3-D QSAR method of comparative molecular field analysis (CoMFA) is applied to the same dataset that was used in the previous Hansch study,⁷ extended by the incorporation of over 20 new compounds, whose synthesis and 5-HT receptor binding are also described. This extended data set is used to develop a common three-dimensional alignment from which CoMFA models are derived, which describe steric and electrostatic requirements for recognition at 5-HT_{1A} and 5-HT₂ receptor sites. It should be noted that the semirigid character of the 4-THPI discussed previously makes them good candidates for CoMFA; since the CoMFA method can only compare single conformations of each molecule in a given analysis, any reduction in the con-

formational degrees of freedom makes finding a common alignment of the molecules easier.

In contrast to the correlation of biological activities with substituent parameters used in Hansch analysis, CoMFA correlated the biological activities of molecules with their steric and electrostatic fields sampled at points in a lattice or grid spanning a three dimensional region around the molecule. Each CoMFA descriptor column of the QSAR table contains the magnitude of either the steric or electrostatic potential, exerted by the atoms in a molecule on the probe atom, located at a point in the Cartesian space surrounding the aligned molecules. The data set so generated is analyzed by the partial least squares (PLS) method which, unlike multiple linear regression, permits the analysis of tables with many more columns than rows. The statistical technique of cross-validation is used to check the validity of model equations which correlate the biological or dependent property with the physical pa-

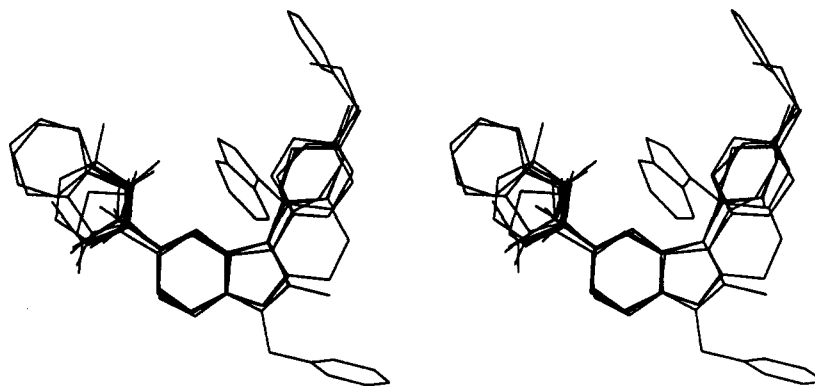


Figure 1. Stereoview of the alignment of the entire set of 4-THPI analogs from Table I.

rameters of the drug molecules. Cross-validation tests a model by omitting compounds (rows), rederiving the model and then predicting the activity of the omitted compounds, thus simulating the prediction of the "real world" outside the training set. As a result of these statistical analyses, a model is derived which explains the activity in terms of 3-D structural properties of drug molecules and is optimized for predicting the biological activity of new analogs. It has been shown that a cross-validated r^2 ($CV-r^2$) of 0.3 corresponds to a probability of chance correlation with activity of less than 0.05 (i.e. $p < 0.05$); hence a $CV-r^2$ value of 0.3 or more is considered significant.^{8,9} The final r^2 is calculated by fitting target properties of all the rows in a table. It is harder to predict values which are not used in deriving a model than it is to fit the same values while including them in a model; thus the cross-validated r^2 will always be much lower than the conventional r^2 for the same data. Usually s is the uncertainty remaining after the least-squares fit has been performed, but in cross-validation, s becomes the uncertainty in prediction over all the compounds, often called "press". As implemented in SYBYL, PLS uses the crossvalidation principle to control its central loop, the iterative derivation of successive components. With each new component, the press is recomputed. The optimum number of components corresponds to the highest cross-validated r^2 .

The present study includes the synthesis and receptor binding studies of the compounds 27–45 and 3-D QSAR analyses of a combined data set of 45 4-THPI analogs (Table I). Since the substituents at the indole 5-position are of prime interest, a total of 27 different indole 5-substituents (Table I) have now been synthesized and studied by molecular modeling. Because of their comparative ease of synthesis, most of the compounds have a methyl or an *n*-propyl group on the pyridine nitrogen; however, a few analogs are unsubstituted at this position (including the lead compound 1). Two of the compounds have a methyl group at the indole 2-position, which were synthesized in order to study the effect of forcing the tetrahydropyridine ring out of the plane of the indole ring.^{7,10} In addition, analogs having a benzyl substituent on the indole 1-position or on the pyridine nitrogen were also examined.

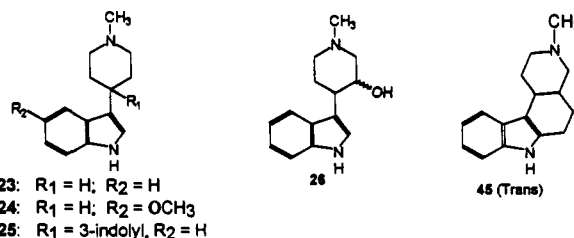
Finally, as a comparison of the relative merits of the predictive capabilities of the CoMFA and Hansch methods, we have derived CoMFAs for 5-HT_{1A} and 5-HT₂ activity from the same set of 5-substituted THPI analogs that we used previously to derive QSAR eqs 4 and 6 in Taylor *et al.*⁷ Both the Hansch and CoMFA methods were then used to predict the activity of 12 of the new compounds with varied 5-substituents; our binding data on these new compounds permits an assessment of the quality of actual

predictions of activity by both methods, which turn out to be about the same, as assessed by the root mean square (rms) residuals between the actual and predicted pK_i values.

Methods

Molecular Modeling and Structure Alignment.

The entire set of THPI analogs listed in Table I were modeled with SYBYL 5.5 (Tripos Associates, St. Louis, MO). Low-energy conformations were determined by molecular mechanics with systematic search of torsional space (MAXIMIN, SEARCH and GRID options of SYBYL), using the unmodified TRIPOS molecular mechanics force field.¹¹ Atomic charges were calculated for the protonated amines using the MNDO method. The unsubstituted 4-THPI analog 4 was first modeled using the standard building options of SYBYL. The preferred conformation of the tetrahydropyridine ring was determined by GRID search, which was then joined to an indole ring taken from a tryptophan residue in the SYBYL protein database. A GRID search was then performed on the rotatable bond between the indole and tetrahydropyridine rings. The lowest energy 4-THPI conformer was selected and used to build the rest of the 4-THPI series for the present study, except for the 2-methyl analogs 20 and 21 and the saturated analogs 23 and 24. Separate conformational analyses (as described above for 4) were performed for these analogs, where deviation from coplanarity was expected. For all of the analogs modeled, independent systematic searches were performed for the various substituent groups in order to determine their preferred orientations.



The common pharmacophore portion, comprising the 4-THPI moieties, were aligned from all the molecules by a least-squares fit on three common atoms: the indole 5-carbon, the indole N-1-nitrogen, and the amino nitrogen. Although, except for the amino nitrogen, this choice of atoms for the fit is somewhat arbitrary, it produces a reasonable overlap of the indole rings while at the same time allowing for any adjustments necessary to more closely superimpose the amino nitrogens (Figure 1). Low-energy conformers of the various substituents at the indole

Table II. 5-HT Binding Data with Hansch and CoMFA Predictions for 3-(Tetrahydropyridin-4-yl)indole Derivatives

compd	LOGP	V ₅	pK _i value									
			5-HT _{1A}					5-HT ₂				
			Hansch analysis			CoMFA		Hansch analysis			CoMFA	
actual	pred	resid	pred	resid	actual	pred	resid	pred	resid			
27	2.288	32.2	7.638	7.689	+0.051	7.761	-0.123	5.867	5.617	-0.250	5.787	-0.080
28	1.808	22.7	6.900	7.818	+0.918	7.760	+0.860	5.762	5.451	-0.311	5.301	-0.461
29	2.338	39.2	6.565	7.568	+0.912	7.481	+0.825	5.509	5.465	-0.044	5.648	+0.139
30	2.868	56.1	6.728	7.276	+0.548	7.476	+0.748	5.291	5.469	+0.178	6.231	+0.940
31	1.868	42.9	7.114	7.504	+0.394	7.097	-0.017	5.000	4.937	-0.063	5.966	+0.966
32	1.658	55.1	6.157	7.293	+1.136	7.050	+0.893	4.272	4.405	+0.133	4.918	+0.646
33	3.448	33.2	7.638	7.672	+0.034	7.677	+0.039	6.921	6.635	-0.286	5.746	-1.175
34	1.258	40.0	6.983	7.554	+0.571	7.602	+0.619	5.616	4.468	-1.148	6.127	+0.511
35	1.208	44.4	6.726	7.478	+0.752	7.630	+0.904	5.760	4.300	-1.460	5.971	+0.211
36	5.428	77.9	6.783	6.899	+0.116	7.208	+0.425	6.662	7.167	+0.505	6.380	-0.282
37	2.640	53.1	7.056	7.328	+0.272	7.289	+0.233	6.695	5.347	-1.348	7.108	+0.413
44	4.798	64.8	7.260	7.271	+0.011	7.060	-0.200	5.957	6.965	+1.008	5.162	-0.795
rms residuals					0.61	0.60	0.75	0.65				

5-position were chosen for optimal overlap with one another, under the assumption that the substituent at this position always occupies the same cavity in the receptor. In our experience, CoMFA simply fails to find a significant correlation if such an approach is not used, e.g. if the global energy minima of a set of various side chains are used (see Discussion).

3-D QSAR Studies by the CoMFA Method. (1) The CoMFA option is SYBYL/QSAR was used to develop a 3-D QSAR for the present set of 45 5-HT₂ ligands listed in Table I. Electrostatic (coulombic) and steric (Lennard-Jones) potentials were sampled for a grid of points in space around the set of molecules, and evaluated as interactions with a probe sp³ carbon atom having a charge of +1. The CoMFA grid spacing was 2 Å in all three dimensions within the defined region, which extended beyond the van der Waals envelopes of all the molecules. The default distant-dependent dielectric model was used for the electrostatic potential calculations. A table was built with the compounds as rows and having two types of column values: 5-HT_{1A} and 5-HT₂ pK_i values (dependent variables) and the steric and electrostatic field potential values (independent variables). PLS analysis runs produced model equations explaining the target property in terms of the independent variables. The optimum number of components in the final PLS model was determined by cross-validation, which also yields a cross-validated r² value. The default value of five cross-validation group was used. Plots of the CoMFA steric and electrostatic fields around the molecules permit the visual properties which determine the pK_i's.

(2) From a subset consisting of 15 4-THPI analogs (4-18, marked with an asterisk (*) in Table I) which vary only in their 5-substituent, Taylor *et al.*⁷ derived QSAR eqs 4 and 6:

$$pK_i = 6.9169 + 0.0400V_5 - 0.0573 \log(10^{(v_5-23.2)} + 1) \quad (\text{for } 5\text{-HT}_{1A} \text{ p}K_i) \quad (4)$$

$$pK_i = 4.4575 - 0.0281V_5 + 0.9022 \log P \quad (\text{for } 5\text{-HT}_2 \text{ p}K_i) \quad (6)$$

We have used these previously derived equations to predict the activity of 12 of our new compounds, 27-37 and 44, which also vary only in their indole 5-substituent (indicated) by double dagger (‡) in Table I). In order to compare the predictive ability of CoMFA vs Hansch analysis, the pK_i values for the above mentioned 12 compounds (27-37 and 44) and were also predicted from

a separate CoMFA derived from the same subset of 15 4-THPI analogs (4-18). It should be noted that there are several reasons why this comparison was performed using the above eq 4 and 6 rather than eqs 5 and 7 from Taylor *et al.*,⁷ which were the "best" reported equations, including a minor electronic component, with r² values around 0.88 as opposed to around 0.75 for eqs 4 and 6. A portion of that electronic component involved atomic charges determined by the CNDO method, which are not directly comparable to the MNDO charges from the present study; furthermore, the strong collinearity (r = -0.85; see table 7 of ref 7) between the two components (Q₅ and R) of the electronic contribution to eqs 5 and 7 suggests that they may be less robust than the simpler eqs 4 and 6, which we have used here. Table II shows a comparison of the predictions from the Hansch and CoMFA methods, using the identical training and test sets described above.

(3) In order to test the predictive capability of CoMFA without the restriction of limiting the training set to compounds that could be treated in a Hansch analysis, a set of six novel 4-THPI analogs (whose syntheses will be reported elsewhere) were modeled and aligned as described above for the set of 45 molecules. The large CoMFA table was appended to incorporate the six new molecules (modeled and aligned as described for the rest of the 4-THPI analogs), without the pK_i values of the new molecules. The values for the six new rows were calculated for the CoMFA column using the EVALUATE option. The pK_i values for the new compounds were then predicted with the QSAR-Analysis PREDICT option (Table III).#

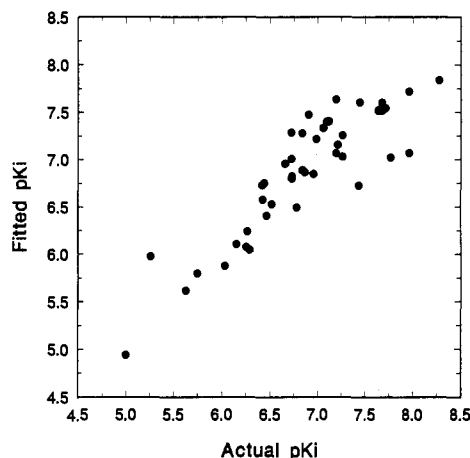
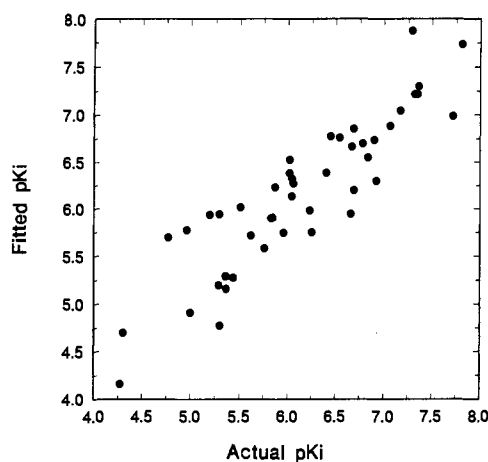
Results

Structure Alignment. Figure 1 shows the alignment of the entire set of 4-THPI analogs listed in Table I.

CoMFA on the Complete Set of 4-THPI Analog Listed in Table I. The optimal number of components for 5-HT_{1A} and 5-HT₂ models were 4 and 5, respectively, with cross-validated r² values of 0.454 and 0.407, respectively. The conventional r² value for the 5-HT_{1A} model was 0.849, with s = 0.29 and F_(4,41) = 57.64, p = <0.001. The conventional r² value for the 5-HT₂ model was 0.840, with s = 0.37 and F_(5,40) = 41.90, p = <0.001. The steric potential seems to be the major contributor for the pK_i's, since 87.3% and 76.5% of the 5-HT_{1A} and 5-HT₂ activities, respectively, are explained by the steric factor alone. Scatter plots of fitted vs actual pK_i values for the 5-HT_{1A} and 5-HT₂ data are shown in Figures 2 and 3.

Table III. 5-HT Binding Data and CoMFA Predictions for Additional 5-Aryl-3-(tetrahydropyridin-4-yl)indole Derivatives

compd	substituents				actual vs predicted pK_i values					
	R	R ₁	R ₂	R ₃	5-HT _{1A}	PRED _{1A}	RESI	5-HT ₂	PRED ₂	RESI
46	H	H	2-thienyl	CH ₃	7.721	6.986	-0.735	6.007	6.045	+0.038
47	H	H	3-thienyl	CH ₃	7.602	7.194	-0.408	5.967	5.919	-0.048
48	H	H	4-fluorophenyl	CH ₃	7.161	7.007	-0.154	5.890	6.262	+0.372
49	H	H	2-pyridyl	CH ₃	7.602	7.039	-0.563	5.552	5.980	+0.428
50	H	H	3-pyridyl	CH ₃	6.699	7.128	+0.429	5.772	5.921	+0.149
51	H	H	4-pyridyl	CH ₃	7.128	7.151	+0.023	5.537	6.191	+0.654
rms residuals							0.46			0.36

Figure 2. Plot of actual vs fitted pK_i values for 5-HT_{1A} activity (data from Table I): $n = 45$; $r^2 = 0.849$; $s = 0.29$; $p < 0.001$.Figure 3. Plot of actual vs fitted pK_i values for 5-HT₂ activity (data from Table I): $n = 45$; $r^2 = 0.840$; $s = 0.37$; $p < 0.001$.

CoMFA for the Subset of 15 4-THPI Analogs Varying Only in Their 5-Substituent. The optimal number of components for these analyses of 5-HT_{1A} and 5-HT₂ models were 2 and 5, respectively, with cross-validated r^2 values of 0.521 and 0.621, respectively. The final analysis gave a conventional r^2 of 0.722, $s = 0.26$ and $F_{(2,12)} = 15.62$, $p < 0.001$ for 5-HT_{1A} activity; the conventional r^2 for 5-HT₂ activity was 0.930, $s = 0.29$ and $F_{(5,9)} = 23.78$, $p < 0.001$. Consistent with the results for the larger data set, 5-HT₂ as well as 5-HT_{1A} activities are explained primarily in terms of the steric potential: the steric contribution to the 5-HT_{1A} and 5-HT₂ activities was 86.8% and 75.9%, respectively.

The results of a CoMFA are best interpreted as CoMFA electrostatic and steric field graphs. These graphs show regions in the space around the molecules as crosshatched contoured volumes, where specific steric or electronic interactions enhance or detract from the activity. In general, the presence of bulk in the green regions in the

steric field graphs contribute positively to the activity while in the red regions detract from the activity. A positive potential in magenta regions and negative potential in yellow regions of the electrostatic field graphs contribute to the activity.

Figures 4 and 5 represent the steric and electrostatic field graphs generated from the CoMFAs of Table I, around the most potent 5-HT_{1A} site active compound, the 5-CONH₂ analog.⁷

Figure 6 and 7 represent the steric and electrostatic field graphs generated from the CoMFAs of Table I, around the relatively more potent and selective 5-HT₂ site active compounds, 7, 19, and 22.

Both types of graph (Figures 4–7) were contoured at the 70 ± 5% and 30 ± 5% contribution levels for the positive (green and magenta) and negative (red and yellow) contours, respectively.

Table II compares the pK_i value predictions for 12 of the new compounds (marked with double dagger (‡) in Table I) by both the Hansch and CoMFA methods, using the small training set of 15 compounds (marked with an asterisk (*) in Table I). The rms residuals for the pK_i predictions at the 5-HT_{1A} site are 0.61 and 0.60 from the Hansch and CoMFA methods, respectively. The rms residuals for the pK_i predictions at 5-HT₂ site are 0.75 and 0.65 from the Hansch and CoMFA methods, respectively.

Table III gives the predicted pK_i 's for six new compounds, using the CoMFAs derived from the complete data set reported in Table I. These values are compared to the actual pK_i 's; the rms residuals for the 5-HT_{1A} and 5-HT₂ predictions for these six compounds are 0.46 and 0.36, respectively.

Discussion

The CoMFA field graphs show regions where variations in the structural features of different molecules in a data set lead to increases or decreases in the target property. They do not emphasize the importance of common structural features of the molecules, because the program can only correlate activity with differences between compounds. An important example is the positively charged basic amino group which is common to all the molecules in the present data set. Although important, and in fact essential for activity, this region of positive potential is not shown in any of the field graphs generated by CoMFA.

Our molecular mechanics calculations suggest that the tetrahydropyridine moiety has a greater tendency to be out of the indole plane when the indole 2-H is replaced by a 2-methyl substituent (20 and 21). This substitution reduces affinity at both the 5-HT_{1A} and 5-HT₂ receptor sites. However, as mentioned above, replacement of the tetrahydropyridine by a saturated ring (piperidine) also

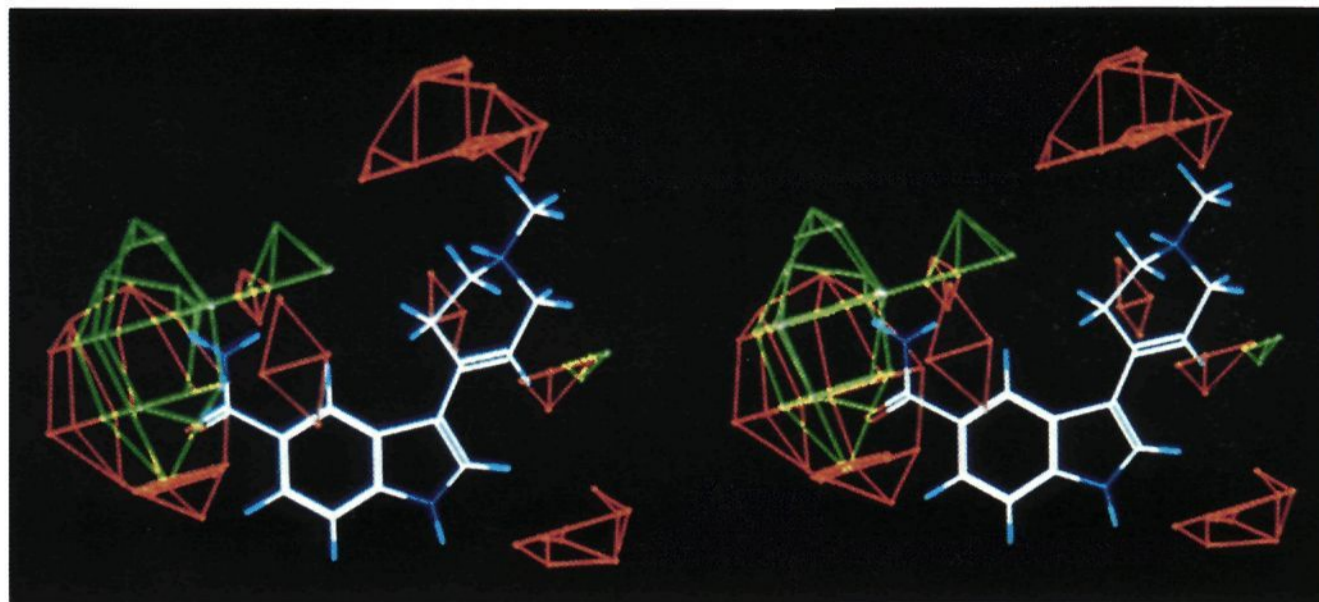


Figure 4. The CoMFA steric field graph for the 5-HT_{1A} model derived from the data in Table I. The most potent 5-HT_{1A} ligand, 14, is shown as reference. This graph shows that 5-substituent bulk approximately the size of a carboxamido group (green region) is optimal for 5-HT_{1A} activity, whereas an out of plane bulk around the indole 5-position (red region) decreases the activity. In addition, bulk beneath the indole 1-position, above the tetrahydropyridyl N-1'-position, and on either side of the tetrahydropyridine ring (red regions) detracts from activity.

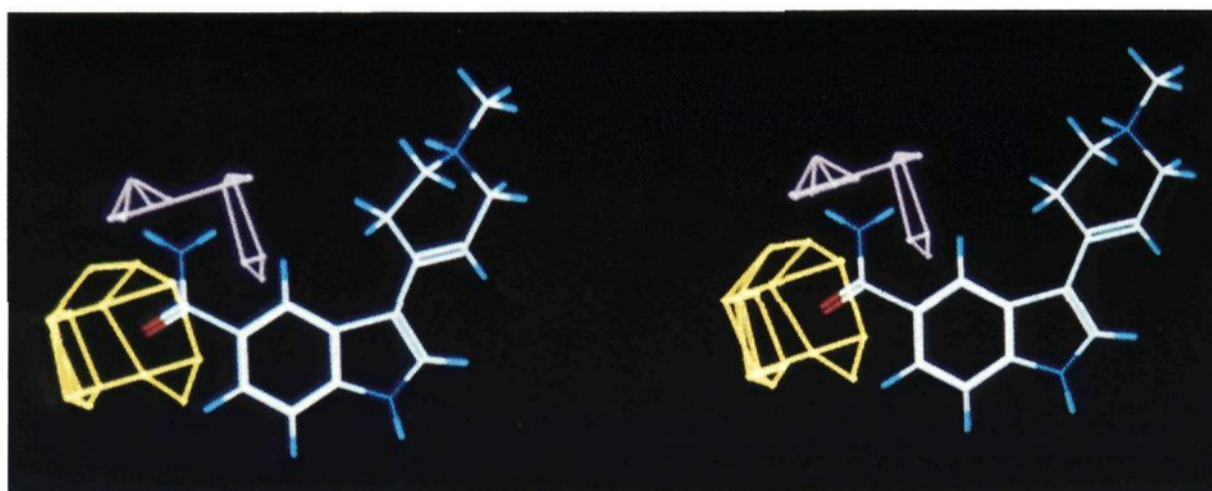


Figure 5. The CoMFA electrostatic field graph for the 5-HT_{1A} model derived from the data in Table I. The most potent 5-HT_{1A} ligand, 14, is shown as reference. The yellow volume in this graph, around the indole 5-position, indicates a region where the presence of negative potential contributes to 5-HT_{1A} activity. A magenta volume above the indole 5-position shows the region where the presence of positive potential increases activity.

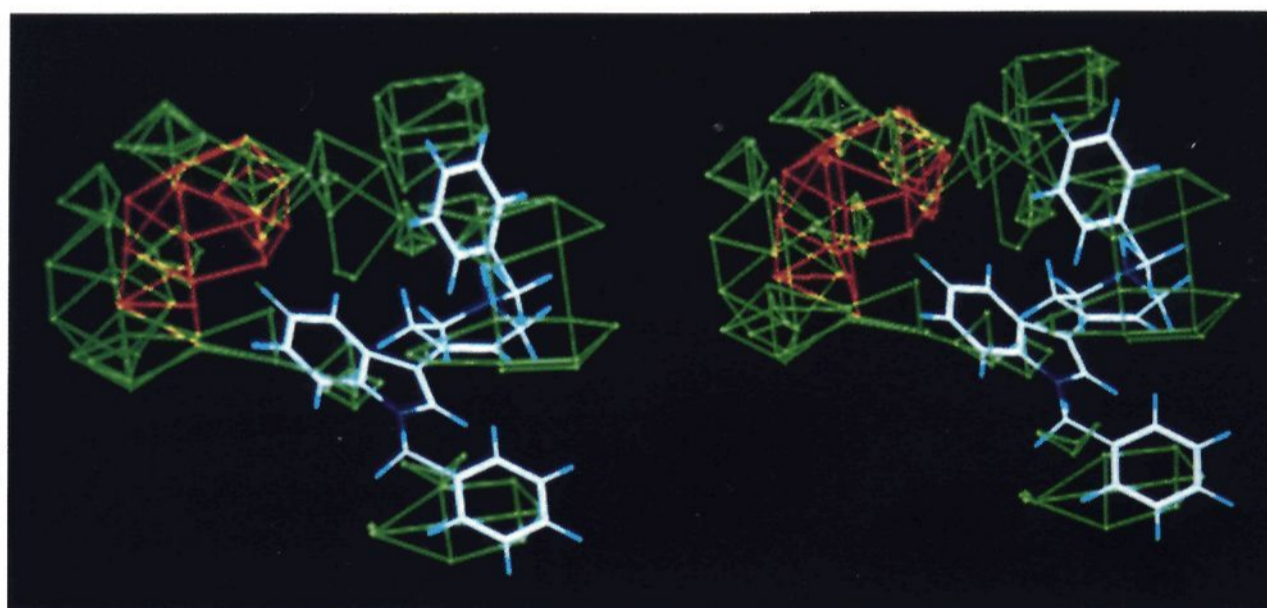


Figure 6. The CoMFA steric field graph for the 5-HT₂ model derived from the data in Table I. Three of the most potent 5-HT₂ ligands, SN-2, SN-12, and SN-13, are shown or reference. This graph shows a red region around the indole 5-position where the presence of bulk decreases 5-HT₂ activity. The green regions spread all around the molecule imply that out of plane bulk generally increases activity.

tends to create noncoplanarity between two systems. From a comparison of the pK_i 's of 4 with 23 and 5 with 24 it seems that the noncoplanarity between piperidine and indole rings acts to increase affinity and selectivity for the 5-HT₂ site; thus the reduced affinity of the 2-methyl analogs 20 and 21 for 5-HT₂ binding may be in part due to other factors, such as steric interference by the 2-methyl group.

The 5-HT_{1A} steric field graph of Figure 4 shows that, for the positions examined, bulky substituents decrease activity except at the indole 5-position (green region where bulk increases activity). In addition, the size of this region is approximately consistent with the previous Hansch analysis, which found the carboxamido group to be of optimal size for 5-HT_{1A} activity. However, it is arguable that it is more difficult to make a quantitative estimation

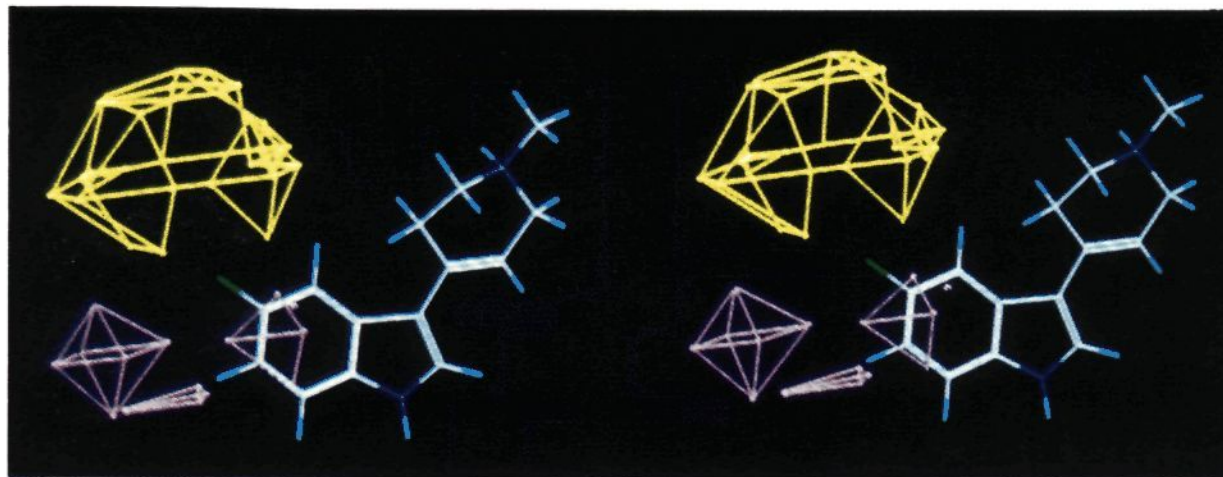


Figure 7. The CoMFA electrostatic field graph for the 5-HT₂ model derived from the data in Table I. Three of the most potent 5-HT₂ ligands, **7**, **19**, and **22**, are shown for reference. The yellow volume above the indole 5-position shows that the presence of negative potential in this region enhances 5-HT₂ activity. In the magenta contoured region above the indole 5- and 6-carbons, and around the indole 6-hydrogen, positive potential contributes to 5-HT₂ binding activity.

or generalization about the optimal size for substituents at this position from these CoMFA results than was possible from the simple bilinear model derived by Hansch analysis (eq 4); nonetheless, the CoMFA model contains more detailed information about the optimal shape of the substituent. The presence of red regions on either side of the indole 5-position implies that bulk in the plane of the indole ring increases 5-HT_{1A} activity, whereas out of plane bulk decreases the activity. Similarly, a preference for near coplanarity of the indole and tetrahydropyridine ring systems is suggested by the red regions (when bulk decreases activity) above and below the plane of the 4-THPI system and a small green region in the plane of the 4-THPI system.

The 5-HT_{1A} electrostatic field graph of Figure 5 shows that, in reference to the potent 5-CONH₂ analog, the presence of negative potential (yellow volume) around the oxygen of the carboxamide group increases 5-HT_{1A} activity of a ligand molecule. In addition, the presence of positive potential (magenta volume) in the region around the amide hydrogens contributes positively to 5-HT_{1A} activity.

Generally, the CoMFA 5-HT₂ steric field graph (Figure 6) is easily understood, clearly showing that bulky substituents at the pyridine N-1 and the indole N-1 positions (the green contoured regions at these two positions) increase 5-HT₂ activity: the latter was not apparent in any of our previous QSAR equations, simply because the N-1 benzyl analog was the only N-1 substituted compound, and had to be omitted from the Hansch analysis. However, the implications for the optimal properties of the indole 5-substituent are more complex. This position is surrounded by an inner hemispherical red region (where bulk decreases activity) which is enclosed by an outer green region (where bulk increases activity). This result implies that a very small or a relatively far situated bulk (particularly if noncoplanar with respect to the 4-THPI skeleton) is optimal for 5-HT₂ activity. In contrast, a substituent that only protrudes into the red contoured region (i.e. a medium sized coplanar substituent) is less favorable for 5-HT₂ activity. It is apparent that this situation is essentially the opposite of that for 5-HT_{1A} where a medium-sized coplanar substituent appears to be optimal. These CoMFA results are reasonably consistent with our previous Hansch analysis, which suggested (1) that a small but hydrophobic 5'-substituent is optimal for 5-HT₂ activity and (2) that in contrast to the decrease in 5-HT_{1A} activity associated with the presence of bulky substituents on the pyridine N-1, the presence of a bulky substituent at this position caused a net increase in 5-HT₂ affinity, by increasing log *P*. Note that the 5-HT₂ activity

(actual p*K*_i 7.36) of the *N*¹-benzyl analog **19** was very well predicted by both CoMFA (7.30, Table I) and the Hansch (7.41)⁷ methods.

The most prominent feature of the CoMFA electrostatic graph for 5-HT₂ (Figure 7) is the yellow region around the indole 5-substituent where negative potential increases 5-HT₂ activity. Consistent with the Hansch analysis of the 5-HT₂ data for these compounds (see ref 7, eq 7), which suggested that positive charge on the indole 5-carbon enhanced activity, a magenta contoured region, where positive potential increases activity, is seen to extend over the indole 5- and 6-positions.

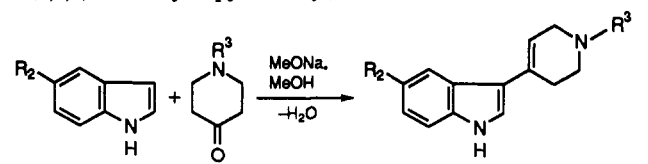
A comparison of the p*K*_i predictions (Table III) from the Hansch and CoMFA methods for 12 of the new 4-THPI analogs, based on an identical training set of 15 previously reported THPI analogs,¹ shows that the predictive capabilities of the Hansch analysis and CoMFA are almost the same for the 5-HT_{1A} data; the CoMFA predictions for 5-HT₂ activity were slightly better than those from the Hansch analysis. However, an obvious advantage of CoMFA is that, unlike Hansch analysis, it permits the incorporation of structurally unique analogs (such as the indole "dimer" **25**) that had to be omitted from the Hansch analysis.

Finally, we used our CoMFA models to predict the activity of six new compounds (Table III) having heteroaryl substituents at the indole 5-position. Although no such 5-heteroaryl-substituted analogs were included while deriving the CoMFA model, the p*K*_i value predictions for the six new compounds are very close to the limits of experimental error. These predictions are significantly better than those from the set reported in Table II, which is to be expected since the training set from which the CoMFA models were derived was 3 times as large (45 vs 15 compounds).

In summary, a number of comments can be made about the relative merits of CoMFA as opposed to Hansch analysis (and vice versa), and in regard to procedural considerations and caveats involved in performing CoMFA on a set of partially flexible molecules, as we have done in this study.

It is apparent that, at least in this case, CoMFA appears to replicate many of the specific results regarding steric factors that were obtained previously by Hansch analysis on a related series of compounds. However, where the properties of a given substituent might have been modeled by a combination of steric and hydrophobic parameters in conventional QSAR (which are usually collinear to a significant degree), the current implementation of CoMFA must produce a model based on steric and electrostatic

Table IV. Physical Data for 3-(1,2,5,6-Tetrahydropyridin-4-yl)indoles

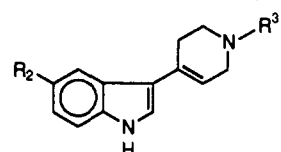


compd	R ₂	R ₃	mp, °C	% yield	formula ^a	analysis ^a
27	COCH ₃	CH ₃	213–215	36	C ₁₆ H ₁₈ N ₂ O	C, H, N ^b
28	CH ₂ OH	CH ₃	186–188	89	C ₁₅ H ₁₈ N ₂ O	C, H, N
29	CH(OH)CH ₃	CH ₃	195–198	68	C ₁₆ H ₂₀ N ₂ O	C, H, N
30	C(OH)(CH ₃) ₂	CH ₃	202–206	86	C ₁₇ H ₂₄ N ₂ O	C, H, N
31	NHCOCH ₃	CH ₃	219–222	56	C ₁₆ H ₁₉ N ₂ O	C, H, N ^c
32	NHSO ₂ CH ₃	CH ₃	236–238	9	C ₁₅ H ₁₉ N ₂ O ₂ S	C, H, N
33	SCH ₃	CH ₃	236–238	90	C ₁₅ H ₁₈ N ₂ S	C, H, N
34	SOCH ₃	CH ₃	214–216	66	C ₁₆ H ₁₈ N ₂ OS	C, H, N
35	SO ₂ CH ₃	CH ₃	242–245	20	C ₁₈ H ₁₈ N ₂ O ₂ S	C, H, N
36	Si(CH ₃) ₃	CH ₃	219–233	53	C ₁₇ H ₂₄ N ₂ Si	C, H, N
37	2-dioxanyl	CH ₃	245–250	35	C ₁₈ H ₁₇ NO ₄ S	C, H, N ^d
38	H	C ₃ H ₇	136–137 ^c	26	C ₁₆ H ₂₀ N ₂	C, H, N
39	OCH ₃	C ₃ H ₇	168–170 ^c	48	C ₁₇ H ₂₂ N ₂ O	C, H, N
40	CONH ₂	C ₃ H ₇	214–217	50	C ₁₇ H ₂₁ N ₃ O	C, H, N
41	CO ₂ CH ₃	C ₃ H ₇	161–163	17	C ₁₈ H ₂₂ N ₂ O ₂	C, H, N
42	CN	C ₃ H ₇	185–187	47	C ₁₇ H ₁₉ N ₃	C, H, N
43	NHCOCH ₃	C ₃ H ₇	187–189	44	C ₁₈ H ₂₃ N ₃ O	C, H, N
44	C ₆ H ₅	CH ₃	221–222	72	C ₂₀ H ₂₀ N ₂	C, H, N
46	2-thienyl	CH ₃	225–227	85	C ₁₈ H ₁₈ N ₂ S	C, H, N
47	3-thienyl	CH ₃	231–234	79	C ₁₈ H ₁₈ N ₂ S	C, H, N
48	4-fluorophenyl	CH ₃	230–232	75	C ₂₀ H ₁₉ FN ₂	C, H, N
49	2-pyridyl	CH ₃	208–210	76	C ₁₉ H ₁₉ N ₃	C, H, N
50	3-pyridyl	CH ₃	240–242	72	C ₁₉ H ₁₉ N ₃	C, H, N
51	4-pyridyl	CH ₃	259–260	82	C ₁₉ H ₁₉ N ₃	C, H, N

^a Combustion analysis were performed for C, H, and N only; experimental values are within 0.4% of theoretical unless otherwise indicated. ^b C: calcd, 75.56; found, 75.15. ^c Analysis values for the hemihydrate (1/2 H₂O). ^d C: calcd, 71.81; found, 71.22.

factors alone. It should be noted that we did attempt adding log *P* as an additional PLS variable in our analyses, but this did not lead to a significant improvement in the

Table V. Analytical Data for New 5-Substituted 3-(1-Alkyl-1,2,5,6-tetrahydropyridin-4-yl)indoles



compd	R ₂	R ₃	mp, °C	% yield	calcd			found		
					C	H	N	C	H	N
42	CN	C ₃ H ₇	185–187	47	76.95	7.22	15.83	76.60	7.37	15.69
41	CO ₂ Me	C ₃ H ₇	161–163	17	72.46	7.43	9.39	72.48	7.45	9.37
38	H	C ₃ H ₇	136–137	26	79.96	8.39	11.65	79.80	8.44	11.57
40	CONH ₂	C ₃ H ₇	218–221	50	72.06	7.47	14.83	72.04*	7.45	14.46
39	OCH ₃	C ₃ H ₇	168–170	48	<i>a</i>					
43	NHCOCH ₃	C ₃ H ₇	187–189	44	70.89 [†]	8.04 ^b	13.41 ^b	70.98	8.02	13.52
36	Si(CH ₃) ₃	CH ₃	219–223	53	71.78	8.50	9.85	71.97	8.45	9.87
30	C(OH)(CH ₃) ₂	CH ₃	203–206	86	70.80	8.39	9.71	70.85	8.51	9.69
28	CH ₂ OH	CH ₃	186–188	89	74.35	7.49	11.56	73.88	7.52	11.42
32	CH ₃ SO ₂ NH	CH ₃	236–238	9	58.99	6.27	13.76	58.11	6.36	13.47
29	CH(OH)CH ₃	CH ₃	195–198	68	74.97	7.86	10.93	74.92	7.90	10.97
27	COCH ₃	CH ₃	213–215	36	75.56	7.13	11.01	75.15	6.89	10.73
37	2-dioxolanyl	CH ₃	245–250	35	71.81	7.08	9.85	71.22	7.03	9.73
33	SCH ₃	CH ₃	236–238	90	69.73 ^a	7.02	10.84	69.38*	6.96	10.73
35	SO ₂ CH ₃	CH ₃	242–245	20	62.04	6.25	9.65	62.04	6.16	9.13
31	NHCOCH ₃	CH ₃	219–222	56	71.35	7.11	15.60	71.17	7.21	15.42
34	SOCH ₃	CH ₃	214–216	66	79.21	6.96	8.80	79.09	7.04	8.84
44	C ₆ H ₅	CH ₃	221–222	72	83.30	6.99	9.71	83.50	6.92	9.71
46	2-thienyl	CH ₃	225–227	85	73.43	6.16	9.51	73.28	6.12	9.26
47	3-thienyl	CH ₃	231–234	79	73.43	6.16	9.51	73.84	6.30	9.44
48	4-fluorophenyl	CH ₃	230–232	75	78.40	6.25	9.14	78.88	6.25	9.21
49	2-pyridyl	CH ₃	208–210	76	78.86	6.62	14.52	78.75	6.62	14.27
50	3-pyridyl	CH ₃	240–242	72	78.86	6.62	14.52	78.56	6.82	14.56
51	4-pyridyl	CH ₃	259–260	82	78.86	6.62	14.52	78.99	6.58	14.58

^a Known. ^b 1/2 CH₃OH.

results. Furthermore, both methods appear to indicate that electronic contributions to activity in this series are rather minor compared to other factors. However, it is arguable that CoMFA provides more detailed information about desirable electronic properties than were attainable through Hansch analysis.

We are inclined to agree with Cramer and co-workers¹⁶ that one must guard against an overly literal three-dimensional interpretation of CoMFA field graphs as a "receptor map". This is particularly true when, in the absence of any independent corroborating information, a rotatable side chain has been placed in an essentially arbitrary position that may correspond to an energy minimum, but not necessarily to an unknown receptor-bound conformation (for example, the orientation of the *N*'- and *N*¹-benzyl substituents of compounds 19 and 22 in this data set). In this situation, we believe that it is particularly important to maintain consistency within a CoMFA study, by choosing rotamers of corresponding side chains to maximize overlap (as we have done here with the 5-substituents, and also in a recent study of kynureninase inhibitors¹⁷), so that the program will be able to compare equivalent moieties in the different molecules, unless there is a strong conformational preference prohibiting an overlapping conformation (e.g. for the piperidine vs tetrahydropyridine ring orientations in this series). This requirement of overlap of analogous substituents sometimes requires rather arbitrary decisions, which can be viewed as a definite shortcoming of the CoMFA method, and at worst provides the potential for a molecule to be twisted into an improbable high energy state that nonetheless aligns with the others, providing a disturbing ability to force a fit to the model that is not possible in conventional QSAR. However, if one at least uses local energy minima for such alignments, as we have done, this

temptation (and high energy conformations) can be avoided, and the number of conformers to be considered is greatly reduced.

On average, neither CoMFA nor the Hansch method appears to give noticeably better or worse predictions of the activity of new compounds, based on our comparison using identical data sets. Since all QSAR methods give better predictions with larger training sets, a clear potential advantage of CoMFA is its ability to incorporate all the available data, and even for data sets on different structural templates to be merged, when appropriate. However, when it can be used, the Hansch approach is certainly procedurally less difficult and less prone to arbitrariness in its implementation.

Experimental Section

Chemistry. Melting points were determined on a Thomas-Hoover capillary melting point apparatus and are uncorrected. 1-Methyl-4-piperidone and 1-*n*-propyl-4-piperidone (Aldrich Chemical Co.) were used without further purification. Those 5-substituted indoles that were not commercially available were prepared and characterized by us previously.^{12,13} The tetracyclic analog 45 was also synthesized earlier in our laboratory.¹⁴ All of the condensation reactions of 5-substituted indoles with either 1-methyl-4-piperidone or 1-*n*-propyl-4-piperidone were carried out in AR-grade methanol (Eastman Chemical Co.) in the presence of an excess of sodium methoxide prepared *in situ*. Physical data for all of the new 5-substituted 3-(1,2,5,6-tetrahydropyridin-4-yl)indoles prepared are summarized in Table IV. The following procedure for the preparation of the phenyl derivative 44 is typical of the reaction conditions employed.

5-Phenyl-3-(1-methyl-1,2,5,6-tetrahydropyridin-4-yl)indole (44). To a solution of NaOMe in MEOH, prepared by reacting 230 mg (10 mmol) of Na in 10 mL of AR-grade MEOH, were added 480 mg (2.5 mmol) of 5-phenyl-1*H*-indole¹³ and 570 mg (5 mmol) of 1-methyl-4-piperidone, and the solution was refluxed for 48 h. The mixture was then cooled and concentrated *in vacuo* (aspirator), and the residue was recrystallized from 95% ETOH to give 520 mg (72%) of a pale yellow crystalline solid, mp 221–222 °C.

5-HT Receptor Binding Assays. These were performed as described previously.⁷ In brief, tissue was obtained from male Sprague-Dawley rats, which were killed by decapitation; the brains were then rapidly removed and dissected over ice. For the 5-HT₁ and 5-HT_{1A} assays, the cortex dorsal to the rhinal sulcus was used; the 5-HT₂ assay was done using frontal cortex alone. Final tissue suspensions were in a buffer of 50 mM Tris at pH 7.6. For the 5-HT₁ assay, [³H]-5-HT to a final concentration of about 2 nM was used as ligand, and unlabeled 5-HT at 10 μM was used to define nonspecific binding. For the 5-HT_{1A} assay, the ligand was [³H]-8-OH-DPAT at about 1 nM, and against 10 μM unlabeled 5-HT was used to define nonspecific binding. [³H]-Ketanserin to a final concentration of about 0.4 nM was used as the 5-HT₂ ligand, and nonspecific binding was defined using 1 μM methysergide. The assay tubes were incubated at 37 °C for 10 min (15 min for the 5-HT₂ assay) and filtered through Whatman GF/B filters using a Brandel cell harvester. For the 5-HT_{1A} and 5-HT₂ assays, the GF/B filters were pretreated with a 0.1%, v/v, solution of poly(ethyleneimine) for 2 h and allowed

to dry (this was found to reduce nonspecific binding to the filters). For a similar reason, the 5-HT₂ assays were performed in disposable polypropylene rather than glass tubes. For all three binding assays, potencies of inhibiting drugs are reported as apparent *K*_i values, calculated from inhibitor IC₅₀ values using the Cheng-Prusoff equation.¹⁶

References

- (1) Euvrard, C. R.; Boissier, J. R. Biochemical assessment of the central 5-hydroxytryptamine agonist activity of RU 24969, a piperidinyl indole. *Eur. J. Pharmacol.* 1980, 63, 65–72.
- (2) Hunt, P.; Nedelec, L.; Euvrard, C.; Boissier, J. R. Tetrahydropyridinyl indole derivatives as serotonin analogues which may differentiate between two distinct receptor types. *Int. Congr. Pharmacol.* 1981, 8, 659, abstr. 1434.
- (3) Hunt, P.; Oberlander, C. The interaction of indole derivatives with the serotonin receptor and non-dopaminergic circling behavior. In *Serotonin-Current Aspects of Neurochemistry and Function*; Haber, B., Ed.; Plenum Press: New York, 1981; pp 547–562.
- (4) Guillaume, J.; Dumont, C.; Laurent, J.; Nedelec, L. (Tetrahydro-1,2,3,6-pyridinyl-4)-3-¹H indoles: synthese, proprietes serotonergique et antidopaminergiques. *Eur. J. Med. Chem.* 1987, 22, 33–43.
- (5) Hoyer, d.; Engel, G.; Kalkman, H. O. Molecular pharmacology of 5-HT₁ and 5-HT₂ recognition sites in rat and pig brain membranes: radioligand binding studies with [³H]5-HT, [³H]8-OH-DPAT, (–)[¹²⁵I]iodocyanopindolol, [³H]mesulergine and [³H]ketanserin. *Eur. J. Pharmacol.* 1985, 118, 13–23.
- (6) Peroutka, S. J. Pharmacological differentiation and characterization of 5-HT_{1A}, 5-HT_{1B}, and 5-HT_{1C} binding sites in rat frontal cortex. *J. Neurochem.* 1986, 47, 529–540.
- (7) Taylor, E. W.; Nikam, S. S.; Lambert, G.; Martin, A. R.; Nelson, D. L. Molecular determinants for recognition of RU 24969 analogs at central 5-hydroxytryptamine recognition sites: use of a bilinear function and substituent volumes to describe steric fit. *Mol. Pharmacol.* 1988, 34, 42–53.
- (8) Clark, M.; Cramer, R. D. III; Jones, D. M.; Patterson, D. E.; Simeroth, P. E. Comparative molecular field analysis (CoMFA). 2. Towards its use with 3-D structural databases. *Tetrahedron Comput. Methods* 1990, 3, 47–59.
- (9) Thomas, B. F.; Compton, D. R.; Martin, B. R.; Seamus, S. F. Modeling the cannabinoid receptor: a three-dimensional quantitative structure-activity analysis. *Mol. Pharmacol.* 1991, 40, 656–665.
- (10) Taylor, E. W.; Nikam, S.; Weck, B.; Martin, A. R.; Nelson, D. L. Relative selectivity of some conformationally constrained tryptamine analogs at 5-HT₁, 5-HT_{1A}, and 5-HT₂ recognition sites. *Life Sci.* 1987, 41, 1961–1969.
- (11) Clark, M.; Cramer, R. D. III; Opdenbosch, N. V. Validation of the general purpose Tripos 5.2 force field. *J. Comput. Chem.* 1989, 10, 982–1012.
- (12) Yang, Y.; Martin, A. R.; Nelson, D. L.; Regan, J. R. Synthesis of some 5-substituted indoles. *Heterocycles* 1992, 34, 1189–1175.
- (13) Yang, Y.; Martin, A. R. Synthesis of 5-arylated indoles via palladium-catalyzed cross-coupling reaction of 5-indolyl-boronic acid with aryl and heteroaryl halides. *Heterocycles* 1992, 34, 1395–1398.
- (14) Herslöf, M.; Martin, A. R. Synthesis of a new conformationally defined serotonin homologue by intramolecular [4+2] cycloaddition. *Tetrahedron Lett.* 1987, 28, 3423–3426.
- (15) Cheng, Y.; Prusoff, W. H. Relationship between the inhibition constant (*K*_i) and the concentration which causes 50 per cent inhibition (IC₅₀) of an enzymatic reaction. *Biochem. Pharmacol.* 1973, 22, 3099–3108.
- (16) Cramer, R. D. III; Patterson, D. E.; Bunce, J. D. Comparative molecular field analysis (CoMFA). 1. Effect of shape on binding of steroids to Carrier Proteins. *J. Am. Chem. Soc.* 1988, 110, 5959–5967.
- (17) Dua, R. K.; Taylor, E. W.; Phillips, R. S. *S*-Aryl-*L*-cysteine *S,S*-dioxides: design, synthesis, and evaluation of a new class of kynureninase inhibitors. *J. Am. Chem. Soc.* 1993, 115, 1264–1270.